

Replication Study and Benchmarking of Real-Time Object Detection Models

Pierre-Luc Asselin¹, Vincent Coulombe², William Guimont-Martin³, and William Larrivée-Hardy³

¹Département de physique, de génie physique et d'optique, Université Laval, Québec, Québec, Canada.

²Département de génie électrique et de génie informatique, Université Laval, Québec, Québec, Canada.

³Département d'informatique et de génie logiciel, Université Laval, Québec, Québec, Canada.

*Authors are presented in alphabetical order, each having equal contribution to the work.

**This report was written in the context of the course GIF-7010 Avancées en apprentissage automatique at Université Laval.

Reproducibility summary

This work examines the reproducibility and benchmarking of state-of-the-art real-time object detection models. As object detection models are often used in real-world contexts, such as robotics, where inference time is paramount, simply measuring models' accuracy is not enough to compare them. We thus compare a large variety of object detection models' accuracy and inference speed on multiple graphics cards. In addition to this large benchmarking attempt, we also reproduce the following models from scratch using PyTorch on the MS COCO 2017 dataset: DETR, RTMDet, ViTDet and YOLOv7. More importantly, we propose a unified training and evaluation pipeline, based on MMDetection's features, to better compare models.

Our implementation of DETR and ViTDet could not achieve accuracy or speed performances comparable to what is declared in the original papers. On the other hand, reproduced RTMDet and YOLOv7 could match such performances. Studied papers are also found to be generally lacking for reproducibility purposes. As for MMDetection pretrained models, speed performances are severely reduced with limited computing resources (larger, more accurate models even more so). Moreover, results exhibit a strong trade-off between accuracy and speed, prevailed by anchor-free models — notably RTMDet or YOLOx models.

The code used in this paper and all the experiments is available in the repository at https://github.com/Don767/segdet_mlcr2024.

1 Introduction

Computer vision, as a machine learning task, has seen unprecedented growth in the last ten years. In 2012, AlexNet showed the proficiency of large convolutional neural networks (CNN) for object detection, leading to increasingly larger and more accurate state-of-the-art CNNs. These models offer great accuracy, but often require significant in-

ference time to obtain predictions. In 2014, R-CNN opened the way to real-time object detection models by limiting inference time while still maintaining competitive accuracy [1]. Since then, different architectures and benchmarks have emerged. This paper wishes to build upon current real-time object detection benchmark methods and reproduce state-of-the-art models.

Object Detection models locate objects of interest in an image or video by identifying the position and boundaries of objects, and classifying them into different categories. As such, typical object detection architecture is divided into three main parts. The *backbone* is used as a feature extractor, giving a feature map representation of the input image. Then, the backbone feeds the feature map to a *neck* which aggregates and produces higher-level features (typically with a feature pyramid network) [2]. The object detection task itself is performed by the *head* on the feature map produced by the backbone and the neck.

When evaluating object detection models, it's tempting to rely solely on metrics like mean Average Precision (mAP) to gauge their performance. While mAP provides a useful summary of a model's precision across different object categories, it's essential to recognize its limitations and consider additional factors in model assessment. mAP focuses solely on detection accuracy and overlooks other crucial aspects such as model speed, resource efficiency, and robustness to real-world variations. A high mAP doesn't necessarily translate to practical usability in some contexts, such as robotics, if the model is too computationally intensive.

This comparative study aims to reproduce a selection of models representative of current techniques in real-time object detection, more specifically YOLOv7 [3], RTMDet [4], ViTDet [5] and DETR [6]. Moreover, an evaluation pipeline was developed in order to fairly compare the different models with each other on precision, frame rate and model size. This pipeline was also applied to a larger selection of models that are already trained so that we can compare them together and draw conclusions.

In order to better compare the different approaches taken for object detection, we offer a review of the three primary approaches as outlined in [7]. Object detection methods mainly follow three approaches: anchor-based detectors, anchor-free detectors, and attention-based detectors.

Anchor-based Detection

Anchor-based methods employ predefined detection boxes, called anchors, to predict object location and size [7]. Two anchor-based methods families are prominent. Models branching from R-CNN are mainly two-stage detectors: first generating proposed regions with a selective search algorithm before doing the object classification task for the selected regions [1]. Other models, such as YOLOv7, are instead single-stage detectors where object classification and bounding-box regression are done directly, without using pre-generated region proposals [3].

A greater quantity of anchors allows such models to better recognize objects of different shapes and sizes, leading to increased performances [8]. However, anchor-based methods demand various hyperparameters to define the anchor box characteristics, burdening training costs and hyperparameter tuning, and thus representing a strong inductive bias. Additionally, anchor-based performances are conditional on how well anchor boxes align with objects and may be limited with overlapping objects [9].

Anchor-free Detection

Anchor-free detectors often utilize feature maps or specific pixel characteristics to predict object locations and sizes. For example, CornerNet detects objects by predicting their geometrical center [10]. This technique removes the need for predefined anchor boxes, thereby enabling the development of lighter and consequently faster models. However, this method relies on more intricate post-processing techniques like thresholding, max pooling, and non-maximum suppression (NMS). Nonetheless, anchor-free detectors require less post-processing time than anchor-based detectors using NMS post-processing and maintain equivalent accuracy [11].

Attention-based Detection

Attention-based architectures, such as Transformers, are originally from the natural language processing (NLP) field but have more recently made breakthroughs in vision tasks [12], due to the advantages of the attention mechanism. Detectors based on transformers remove the need for anchors and feature maps by directly predicting bounding boxes and class labels using the cross-attention mechanism of the transformer with a set of learnt positional embeddings [6]. The transformer encoder uses self-attention to

extract information from the image, and the transformer decoder uses cross-attention between this extracted data and the learnt positional embeddings. The decoder's output embedding is then used by a classification head and a feed-forward network to predict class and bounding box location, respectively. It is important to note that such models use a limited number of detection boxes fixed by the number of learnt positional embeddings. As such, models based on this approach can forgo post-processing steps and directly predict unique bounding boxes [6].

2 Scope of reproducibility and benchmark

No original author was contacted during this work. Implementations were solely based on selected original papers [3–6]. If insufficient information is given in the paper, the official code repository was consulted. Every instance where this was necessary is mentioned explicitly. Additionally, no pretraining method was reproduced. Pretrained weights for the backbones were used when available.

The additional benchmarked models were taken from MMDetection's catalogue of pretrained models. Due to time constraints, we selected an array of models representing state-of-the-art methods. We used these models as provided and ran them in our evaluation pipeline.

3 Methodology

3.1 Metrics

The usability of deep neural networks is not only based on accuracy, but also on model size, inference speed and post-processing load required to use the output. To better capture a model's practicality, the following metrics are measured:

- Mean average precision from 0.5 IoU to 0.95 with 0.05 steps (mAP);
- Average precision at 0.5 IoU (AP50);
- Average precision at 0.75 IoU (AP75);
- Average precision for small objects (APs);
- Average precision for medium objects (APm);
- Average precision for large objects (APl);
- Network size;
- Prediction time for a batch of 1 image (including all required post-processing);
- Prediction time for a batch of 16 image (including all required post-processing); and
- Prediction time for a batch of 32 image (including all required post-processing).

The recorded inference time considers the entire process from input processing to obtaining usable output, ensuring representability of real-world applications. Studying the prediction time across multiple batch sizes is crucial to understand how a model’s performances scales. This is done by estimating amortized inference time, i.e., the average time taken for a batch. This metric could be representative of *almost real-time* tasks where detection need to be done on a small batch of buffered inputs — i.e., scenarios where timely processing of a few consecutive frames is essential.

3.2 Experimental setup and code

Table 1: Hardware used for our study.

Nb	GPU	CPU	RAM
1	Titan X	AMD Ryzen 7 1700	16 Gb
1	Quadro RTX-8000	i7-6700K	32 Gb
4	RTX A6000	AMD Ryzen 3970X	128 Gb
1	RTX-3080 Ti	i7-12700K	64 Gb
1	RTX-4090	i9-13900F	64 Gb

Model training was exclusively made using computing resources at the Northern Robotics Laboratory (NorLab) from Université Laval. GPUs (see table 1) were selected in such a way as to offer a range of performance, memory and release date. Model training was made exclusively with the 4 available A6000 GPUs without any multi-GPU training. Training was made within a Docker environment,¹ using Slurm² for job scheduling. This contributes to standardizing the software stacks while ensuring the possibility to port both training and evaluation to various machines. A unified pipeline simplifies model comparisons on different hardware.

All models listed in section 3.4 were evaluated through this pipeline. Before each evaluation, a few iterations are made to avoid cold starts. First, the precision metrics are evaluated on the validation set of MS COCO 2017 (see 3.3 for more details), followed by a measurement of the total prediction time on all images. This inference time estimation includes any post-processing used by the model, non-maximum suppression for instance. This is done on batch sizes of 1, 16 and 32.

All used code for this reproducibility project is available in the repository at https://github.com/Don767/segdet_m1cr2024 (April 21st 2024).

¹Based on docker image
pytorch/pytorch:2.2.1-cuda12.1-cudnn8-devel

²<https://slurm.schedmd.com/overview.html> consulted April 19th 2024.

3.3 Datasets

For all training and testing, only MS COCO 2017,³ was used. This dataset contains 118K images in its training set and 5K images for validation. All images have bounding boxes and masks over 80 object categories. Reported average precisions are computed using the python library `pycocotools`.⁴

3.4 Models

Four models in real-time object detection were selected for reproduction, based on their performances, but also to be representative of current state-of-the-art approaches.

Yolov7

First introduced in 2015, *You Only Look Once* is a family of real-time object detection algorithms that stands out for its balance of accuracy and speed [13]. The YOLO architecture unifies object detection by trying to detect every bounding box simultaneously, framing the problem as a regression problem instead of a classification problem (by spatially separating bounding boxes and predicting their respective position and probability). This allows YOLO models to give predictions in a single pass of the network. Following iterations of YOLO gradually boosted the architecture’s performances. Since YOLOv2, anchor-based detection is used by this family to further improve accuracy (with the notable exclusion of YOLOx [14] models) [15]. At the time of its release in 2022, YOLOv7 surpassed every other object detection model in both accuracy and speed (for the range of 5 to 160 FPS) [3]. YOLOv7 is largely based on YOLOv5 [16], but incorporates *implicit knowledge* from YOLOR [17]. Implicit knowledge is similar to human past experience knowledge. YOLOv7 therefore uses information on prior tasks for its predictions.

YOLOv7 also includes a *bag-of-freebies*: a series of optional features that increase the model’s accuracy without affecting inference time. These include: a planned re-parametrization of convolution blocks, coarse label assignment in an auxiliary head during training, batch normalization, exponential moving average for the final inference, etc. However, these components do affect training time, as noted by the original authors [3]. The code behind the model is open-source and comes with instructions for out-of-the-box usage with MS COCO 2017.⁵

³<https://cocodataset.org/#home> consulted April 19th 2024.

⁴<https://pypi.org/project/pycoco/> consulted April 19th 2024.

⁵<https://github.com/WongKinYiu/yolov7>, consulted April 19th 2024.

RTMDet

RTMDET (*Real-Time Models for object DETection*) is a single-stage, anchor-free approach to object detection [4]. It leverages innovative architectural features, including wide depth-wise convolution to enhance performances of YOLOx’s architecture [14]. Moreover, RTMDet employs advanced training optimizations such as: diverse augmentation strategies, exponential moving average and dynamic soft label assignments.

A CSPNeXt backbone is introduced to maximize the effective receptive field while ensuring computational efficiency. CSPNeXt is a stack of wide and shallow CSPNeXt blocks. Each block exploits a 5x5 depth-wise convolution, which is identified as the optimal kernel size to expand the receptive field without significant computational overhead [4]. Additionally, CSPNeXt integrates channel-wise attention mechanisms after each stage to reduce the total number of blocks (24 to 18) while maintaining performances.

A multiscale feature pyramid network acts as neck [2], mirroring the same architectural strategy as the backbone. Due to the relatively shallow nature of each feature pyramid scale level, no skip connections are used between its blocks. It is worth noting that the neck’s total parameter count is similar to the backbone’s, as empirical evidence suggests that backbone-neck symmetry yields better performances [4].

The model uses a shared detection head for all scales, which reduces parameter count by approximately 10% without impeding performances [4]. However, each scale within the pyramid does not share the same batch normalization layer, as the statistical characteristics of features differ for each scale [4].

The loss function (equation 1) is composed of a Quality Focal Loss (QFL) [18] and a General Intersection Over Union (GIoU) [19]. The labels are assigned via a novel dynamic soft label assignment strategy, leveraging SimOTA [14] methodology.

$$\mathcal{L} = \lambda_1 \cdot \text{GIoU} + \lambda_2 \cdot \text{QFL} \quad (1)$$

where $\lambda_1 = 2$ and $\lambda_2 = 1$.

The training pipeline uses a similar augmentation strategy as YOLOX such as the usage of MixUp [20] and Mosaic [21] for approximately the initial 90% of the training duration. However, the authors avoided random rotation and shearing, as they cause misalignment between box annotations and the inputs. Regarding optimization, AdamW [22] is preferred over SGD due to empirical evidence indicating unstable convergence progress with

the latter [4], especially when subjected to heavy data augmentation during training. The learning rate starts with a warm-up and remains constant until halfway through training. Subsequently, it transitions to cosine annealing for the latter half.

ViTDet

Typically, object detection heads rely on multiscale feature maps produced from a hierarchical backbone — such is the case for models using ResNet [23] or Swin [24] backbones. Vision Transformers have shown to be powerful visual recognition backbones in image classification, but are rarely used directly in object detection since they are plain and non-hierarchical, and thus, not adapted to most object detection heads [25]. ViTDet proposes the use of Simple Feature Pyramids (SFP) as necks to generate multiscale feature maps that can adapt any backbone network to any detection head — including non-hierarchical backbones. SFP uses a series of simple convolution and deconvolution layers to generate maps of different scales ($\{\frac{1}{32}, \frac{1}{16}, \frac{1}{8}, \frac{1}{4}\}$) using only the single-scale output from a ViT.

ViTDet uses a ViT plain backbone directly with a Cascade Mask R-CNN head. Performances on COCO datasets are competitive with other architectures based on ViT (but adapting it for hierarchical structures) such as Swin, while having faster inference and training times [5]. ViTDet has opened the way to general-purpose backbones, with minimal architecture changes for different tasks. The code used by the original authors is completely open-source.

DETR

DETR (*DEtection TRansformer*) is a transformer-based architecture composed of a CNN backbone, an encoder-decoder pair as a neck and a feed-forward network (FFN) head. Images undergo processing within the CNN backbone, generating a lower-resolution activation map. The typical output dimensions are $C = 2048$ channels of spatial dimensions $(H, W) = (\frac{H_0}{32}, \frac{W_0}{32})$, where (H_0, W_0) is the input’s size. This activation map is then passed through a 1x1 convolution to reduce channel dimension and split into a sequence of patches, before reaching the encoder. Each encoder layer consists of a multi-head self-attention block followed by a FFN. Positional encodings are added to the input at each attention layer to preserve spatial information.

From the input sequence, the decoder generates N output embeddings. These output embeddings make up the input of a 3-layer perceptron with ReLU activation acting as the architecture’s head. This FFN predicts the normalized coordinates and dimensions of the bounding

box, and a linear projection layer predicts the class using a softmax function. A special class label named *No object* is added to represent when a detection does not correspond to an object. This addition is required since the number of predicted boxes is fixed, depending on the learned embedding fed into the decoder. Predicted boxes and labels are assigned to ground truth using Hungarian matching. Finally, the loss is computed by adding an IoU bounding box loss to a classification loss.

Other methods

The open-source MMDetection toolbox⁶ (offered by the OpenMMLab project) provides different pretrained model implementations. Since MMDetection is at the core of our training pipeline, we also considered performances for the following pretrained models: Mask R-CNN R50, Mask R-CNN R101, Mask R-CNN X101, Mask R-CNN Swin, Mask R-CNN Swin (Crop) [26], Faster R-CNN R50, Faster R-CNN Swin, Faster R-CNN X101 [27], DETR, DETR R50 [6], Deformable DETR R50 (2 stages), Deformable DETR R50 [28], Cond. DETR R50 [29], DAB DETR R50 [30], YOLOv3, YOLOv3 d53 [21], MobileNetV2 [31], DINO-5 Swin, DINO-4 R50 [32], YOLOf R50 [33], CenterNet R50 [10], RetinaNet [34], YOLOX-tiny, YOLOX-s, YOLOX-l, YOLOX-x [14], RTMDet-ins tiny, RTMDet-ins m, RTMDet-x and RTMDet [4].

3.5 Implementation details

Model training code uses MMDetection, an open-source object detection toolbox. The rest of this section give additional implementation information for each reproduced model.

Yolov7

The Yolov7 base model was reimplemented using PyTorch modules. We did not use any pretrained weights from the original authors. Additionally, Yolov7's custom data loader, custom loss function and data augmentation were taken directly from the original code repository and not reimplemented from scratch (this required the implementation of a compatible argument parser). No feature from Yolov7's *bag-of-freebies* was used during training or testing. Due to difficulties adapting YOLOv7's data loader to OpenMMLab's architecture, this reproduction is the only one not using MMDetection modules for training. This issue is recognized by OpenMMLab, which provides another toolbox specifically for YOLO family models.⁷ All hyperparameters used are presented in table 7. These hyperparameters

⁶<https://github.com/open-mmlab/mmdetection>, consulted April 21st 2024.

⁷<https://github.com/open-mmlab/mmyolo>, consulted April 25th 2024

match those used for Yolov7's base model. Only the batch size is different, being 64 instead of 32 to accelerate training.

RTMDet

The RTMDet small model was reproduced using the MMDetection [35] toolbox. As such, we did not reimplement the dynamic label assignments with soft labels, the augmentation pipeline, the loss calculation and the post-processing steps including NMS [13], as they were already integrated within the framework. We trained the model on MS COCO 2017 using the hyperparameters presented in Table 7.

ViTDet

The ViTDet base model (ViT backbone with Cascade Mask R-CNN head) was reimplemented as described in the original paper using the MMDetection toolbox. We implemented a custom neck implementing the SFP generating multiscale features from the output of a ViT backbone. This backbone is a ViT pretrained with MAE [36]. The output of the SFP is then fed into a CascadeRoIHead head from MMDetection. While the original paper did not describe the use of any data augmentation pipeline, we opted to replicate the same data augmentation used in RTMDet. All hyperparameters used are presented in table 7. Only the batch size is different from the original paper, being 24 per GPU instead of 1 per GPU.

DETR

The DETR base model was reproduced as described in the original paper [6], the only difference being the batch size used during training (40 instead of 64). As described in the original paper, the PyTorch implementation of Transformers cannot add positional encoding at the input of each layer. Thus, we used the implementation of Transformer from `willGuimont/transformers` [37].⁸ We used the standard pretrained ResNet50 [23] from PyTorch for the backbone.

Pretrained models

For the other considered approaches, we automated the evaluation pipeline as much as possible. First, we parse every model description present in the MMDetection GitHub repository to find all the models providing pretrained weights. We then, due to time constraints, selected an array of methods to benchmark. Our pipeline downloads automatically the configuration file, containing everything needed to reproduce the model in the MMDetection framework, and the corresponding weights. We then run the models

⁸<https://github.com/willGuimont/transformers>, consulted on April 28th 2024

through our unified evaluation benchmark and collect the inference statistics.

4 Results

Our implementation gave poor results for ViTDet and DETR. Section 5 goes into further detail about the different problems we faced with these models. Our implementation of RTMDet achieved comparable results to its original paper, as shown in table 2. While the latency may initially appear to be comparatively low, it should be noted that the FPS reported by [4] does not include post-processing latency. This setup, while facilitating fair comparisons between models with similar post-processing steps, artificially enhances performances of anchor-free models as they are typically used alongside post-processing in practice. Additionally, this unfairly biases against methods such as transformer-based detection, lacking such post-processing steps. Figure 1 shows examples of qualitative results obtained by our implementation of RTMDet on the validation set of MS COCO 2017.

Results obtained for our implementation of YOLOv7 are presented in table 3. Accuracy performances presented in the original article could not be matched by our own implementation. This difference can realistically be associated to the *bag-of-freebies* used in the original article, as this work didn't implement any feature within it. On the other hand, speed performances declared in the original paper could be reproduced, albeit on different hardware, and even exceeded at greater batch size. It is important to note that, as detailed in 5, our implementation of YOLOv7 uses YOLOv7's original testing and training pipeline. Therefore, performances obtained with this implementation should not be compared directly to other results presented in this paper.

Table 2: Model performances (original vs our reproduction) for RTMDet. The values for the original implementation of RTMDet are taken from the original article and do not include time taken by the post-processing steps.

Model	GPU	mAP	FPS
RTMDet [4]	RTX-3090 (FP16)	44.6%	*161.0
RTMDet (ours)	TitanX	44.4%	44.0
RTMDet (ours)	Quadro	44.4%	59.6
RTMDet (ours)	A6000	44.4%	63.1
RTMDet (ours)	RTX-3080Ti	44.4%	129.9
RTMDet (ours)	RTX-4090	44.4%	160.8

Despite not achieving competitive results with our implementations of ViTDet and DETR, we nonetheless report inference times for both models in table 4 and in table 6 respectively.

Table 3: Model performances (original vs our reproduction) for YOLOv7. The values for the original implementation of YOLOv7 are taken from the original article.

Model	GPU	mAP	FPS	Batch Size
YOLOv7 [3]	V100	51.4%	*161	1
YOLOv7 (ours)	RTX-4090	44.6%	232	1
YOLOv7 (ours)	RTX-4090	44.6%	27	16
YOLOv7 (ours)	RTX-4090	44.6%	14	32

ViTDet, after 47 epochs out of the 100 planned, achieved some weak performances, reported in table 5. Although the training process is still ongoing, those partial results still offer valuable insights. Notably, we notice a gradation of the performances with respect to object size. Large objects achieve an average precision of nearly 20%, while medium objects reach around 7%, and small objects only about 1%. This disparity shows the challenge of learning smaller objects compared to larger ones. We further discuss these results in section 5.

The implementation of DETR did not converge and has a mAP of 0%. The rest of this section will focus on the results obtained with the produced testing pipeline on models mentioned in section 3.4 as we feel it is our greatest contribution.

Table 4: Frame per seconds across considered GPU of our ViTDet implementation for a batch size of 32.

GPU	FPS
TitanX	0.2
Quadro	0.7
A6000	1.0
RTX-3080Ti	1.1
RTX-4090	2.0

Table 5: Model performances of our implementation of ViTDet after 47 (out of 100) epochs of training.

Metric	Value
mAP	0.095
AP50	0.186
AP75	0.090
APs	0.010
APm	0.065
API	0.200



Figure 1: Example of results obtained with our reproduced RTMDet on MS COCO 2017.

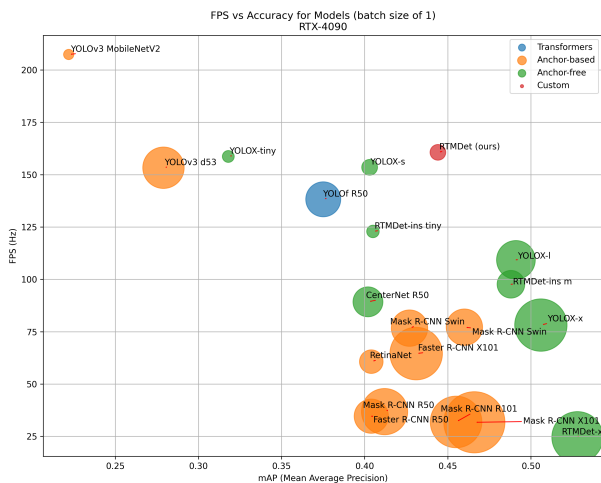


Figure 2: Accuracy and frame rate of different models on RTX-4090 with a batch size of 1.

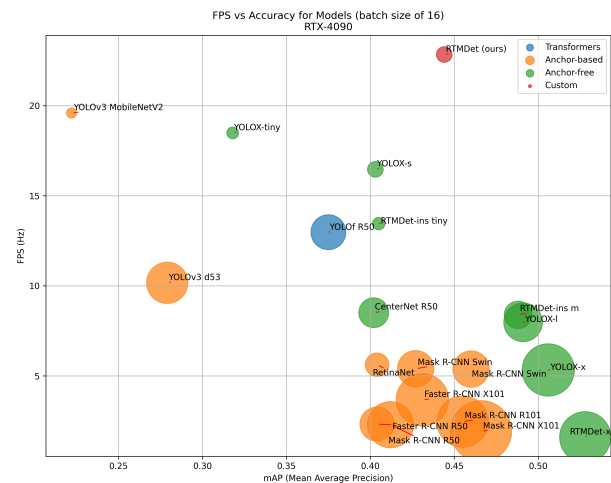


Figure 3: Accuracy and frame rate of different models on RTX-4090 with a batch size of 16.

MMDet pretrained models

We report the performance metrics for pretrained models from MMDetection in appendix B. Table 8 shows frame-per-second performances of selected pretrained models. Various attention-based models’ inference time (DETR and DINO families) could not be estimated properly, those models require more specific data that our pipeline does

Table 6: Frame per seconds achieved by our implementation of DETR on a RTX-4090 across multiple batch size.

Batch size	FPS
1	115.4
16	11.7
32	5.8

not yet fully support. Such models do offer competitive accuracy performances, but, since it is currently difficult for non-industrial users to access hardware similar to the high-end GPUS tested (RTX-4090), common usage of DINO and DETR models (as implemented in MMDetection) for real-time object detection seems impractical because of the memory requirements for transformer based models. For transformer-based models, YOLOf R50 exhibits comparable speed performances to anchor-free and anchor-based architectures.

Table 8 shows improved speed performances for all models when computing resources increase, which is expected. We also provide the achieved mAP on all selected models in table 11.

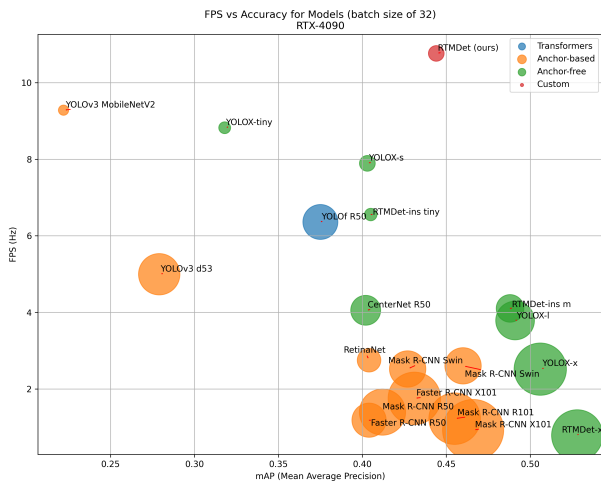


Figure 4: Accuracy and frame rate of different models on RTX-4090 with a batch size of 32.

Additionally, figures 2, 3 and 4⁹ reveals that increasing the batch size reduces speed performances for every model studied. More importantly, not all models seem to be affected in the same way by an increased batch size. Indeed, YOLOx and RTMDet family models maintain better speed performances with an increased batch size than other models tested. Broadly speaking, figures 2, 3 and 4 imply that lighter models are less affected by a larger batch size (large models agglomerate to the bottom of the graphs).

On the flip side, the larger models depicted in the same figure tend to showcase higher levels of accuracy. In essence, the figure illustrates a relative trade-off between accuracy and inference time. Models belonging to the YOLOx and RTMDet families appear to strike a better balance between accuracy and speed compared to other models tested, at least within the range of GPUs examined. This observation extends to our RTMDet implementation, where an aggressive pre-filtering strategy results in lighter and more efficient NMS and thresholding procedures. This approach appears to lead to better-amortized latency, as demonstrated in Figures 3 and 4, emphasizing the crucial role of post-processing in latency measurement.

5 Discussion

Reproducibility

The following considers in more detail the issues linked to the reproducibility of selected benchmark models.

Yolov7

Yolov7 truly shines for out-of-the-box usage. Indeed, code, weights and usage instructions are easily accessible and user-friendly — including both Docker setup instructions

⁹The exact numbers used to generate these graphs are available in appendix B

and Google Colab premade setup. These instructions also include the necessary explanation to use features within the *bag-of-freebies* with Yolov7 premade models.

Yolov7, taken as a product, is an excellent model. However, the same cannot be said for developers: details given within the article and the code repository are insufficient for reproducibility or model customization. First, the article is highly dependent on prior knowledge of previous YOLO-family models. For example, it is mentioned that the architecture is based on YOLOv5's and includes YOLOR's implicit knowledge, but no details are given on how this is implemented (whether in the article or the code repository). Searching previous YOLO papers and architectures (mainly YOLO3 [21], YOLOR [17] and YOLOv5 [16]) is essential to understand and reproduce YOLOv7 from scratch. Other articles are referenced as the source of some code blocks in the code itself (for example, YOLOv7 uses a SPPCSPN¹⁰ layer) but not mentioned within the article or the usage instructions. Additionally, the article neglects important information necessary for the reproduction of training conditions, including the data augmentation and the loss function used.

Moreover, YOLOv7 sometimes neglects to use conventional PyTorch or TensorFlow code structure in favor of made-from-scratch implementations of corresponding functionalities. For example, YOLOv7 uses a custom data loader for its training, a custom data augmentation pipeline and a custom learning rate scheduler. This wouldn't be a problem by itself, but the fact is that YOLOv7's training environment is highly dependent on said custom structure. In that way, it is quite challenging to reuse the same training regiment as YOLOv7 with a custom reimplement of the model. In the same way, YOLOv7's pre-trained weights are defined with a custom pickle¹¹ format instead of pth as commonly used in PyTorch, complexifying its usage outside of YOLOv7's premade architecture, as it depends on having specific Python modules at specific paths. The complexity of reproduction is further exacerbated by the absence of details in the original article for any such custom feature.

Finally, the included *bag-of-freebies* is interwoven within the model's code and acts as a lot of background noise when trying to understand the model itself. Which *bag-of-freebies*' functionalities and with what parameters were used to obtain the results presented in the original paper is also mostly left unanswered. In the end, YOLOv7's training took 8 days.

¹⁰Cross Stage Partial Networks Spatial pyramid pooling layer from <https://github.com/WongKinYiu/CrossStagePartialNetworks>, consulted April 21st 2024.

¹¹<https://docs.python.org/3/library/pickle.html>, consulted April 26th 2024.

RTMDet

The MMDetection toolbox offers an elegant, easily extendable modular design. This characteristic makes it a fitting choice to reimplement not only RTMDet, but most of our selected algorithms. Working within the toolbox conventions enabled us to leverage its rich ecosystem of data processing, data augmentation, loss function and post-processing utilities. Especially for RTMDet, as every tool mentioned in the paper was available directly within the repository, which allowed us to focus on the reimplementation of the model itself.

While MMDetection toolbox’s excellent software engineering practices facilitate easy extensibility, they introduce a significant level of abstraction, making it challenging to locate actual implementations. This, combined with some lack of details in the paper, made some parts of the reimplementation more difficult. Notably, the CSPNeXt backbone is not entirely described in the paper. Furthermore, discrepancies were observed between the actual loss function utilized in the repository and the well-described variant presented in the paper. Curiously, the implementation uses equation 1 as its loss function, which is only briefly described as the baseline in the paper. Training took 7 days and happened without incident.

ViTDet

Some important hyperparameters necessary to reproduce ViTDet were absent in the original paper. First, the paper mentions the usage of a learning rate step during training without further details. Searching the official code repository shows a multiplicative step of 0.1 for iterations 163889 to 177546. Additionally, the original paper does describe the SFP architecture, but omits to mention that the intermediary embedding between convolution and deconvolution layers reduces channel width by half. The article does mention a ViT backbone based on Masked Autoencoder [36], but modifications are made to it in the official code repository for ViTDet which are only briefly mentioned by the original authors. Besides these oversights, reproducibility was mostly uneventful.

The training itself was more time-consuming than expected. At the time of writing this paper, it is still not finished and goes at a rate of 14 iterations per day (on a A6000 GPU). At this rate, the total training time will be more than 7 days. Due to time constraints and occasional divergences in training, it became impossible to complete the entire training schedule planned in the article. Nonetheless, we report the inference time and accuracy of our implementation of ViTDet in tables 4 and 5. The results shown are obtained after 47 epochs. Our implementation achieved a mAP of approximately 10% by

that point, confirming our network is learning, albeit at a prohibitively slow rate for our time constraints.

DETR

DETR is conceptually simple and paired with a well-detailed article. Reproduction using exclusively the original paper is achievable. Notably, the batch size had to be adjusted to 40 instead of 64 due to memory limitations. Otherwise, hyperparameters (see table 7) presented in the article were used directly. However, issues arose at training. After the intended 300 epochs (6 days of training time), the network always predicted the *No object* label. Looking at the official code, a few omissions within the paper were found. First, the normalization layer within the transformers is in reality placed before the attention mechanism instead of after. The positional encoding added to the image is only applied to the non-padded section of the input. We tried implementing these changes, but the network still consistently predicted the *No object* label. In fact, the learning rate schedule used in the original article seem too simple to achieve appreciable results. Pairing this with the lack of data augmentation makes it seem like the training process presented is lacking refinement, which hinders the speed at which the network learns. The model still learns after the 300 epochs originally used, so we are hopeful that we could achieve similar performances to the original paper, but with significantly higher training costs. Nonetheless, we report the inference speed of our implementation in table 6, and found it competitive in terms of inference time.

6 Conclusion

In this work, four state-of-the-art models (YOLOv7, RTMDet, ViTDet and DETR) were selected for reproduction to determine if such models offer sufficient accuracy and speed in a non-industrial environment. Overall, only RTMDet and YOLOv7 could offer significant performances. The two other models were found to be too computationally expansive for our hardware, much more than what could be expected from the original papers. Moreover, papers for YOLOv7, ViTDet and DETR were found to be insufficient for reproducibility purposes, lacking fundamental information on both the architecture or training context.

A unified training and testing pipeline built on MMDetection was produced and used to evaluate 30 different pre-trained models offered by MMDetection. Experimentation showed the trade-offs between model accuracy, speed and size. For the context of real-time object detection, models based on an anchor-free architecture (mostly RTMDet and YOLOx) achieve a better compromise between accuracy, speed and size than tested anchor-based or attention-based models.

Future works could include testing with additional hardware (including Nvidia Jetson and Orin GPUs to investigate the use of these models in embedded settings) using the same unified pipeline. Additional hardware could help to support speed performance estimation for the more demanding architectures (notably DETR and DINO). We also wish to explore the impact of mixed precision on model inference speed. Moreover, MMDetection offers various other models besides those considered in this work, which were initially excluded due to time constraints. Expanding our benchmark to include a wider range of models beyond those available in MMDetection, we aim to incorporate models provided by Hugging Face as well.¹² The built pipeline is found to be flexible and reliable; model benchmarking on a larger scale based on this infrastructure seems to be an achievable step forward for this work. We also aim to test additional models beyond just object detection, such as panoptics, 3D object detection and human pose estimation, with our benchmarking pipeline.

Acknowledgement

We would also like to acknowledge the generous support of NVIDIA Corporation for providing a Quadro RTX 8000 GPU, which enhanced the computational resources used in this research. Thanks to the Northern Robotics Laboratory (norlab)¹³ from Laval University for access to computing resources. Thanks to David-Alexandre Duclos for allowing us to use his TitanX GPU.

References

- [1] R. Girshick, J. Donahue, T. Darrell and J. Malik. “Rich feature hierarchies for accurate object detection and semantic segmentation”. *arXiv* (2014).
- [2] T.-Y. Lin, P. Dollár and al. “Feature Pyramid Networks for Object Detection”. *arXiv* (2017).
- [3] C.-Y. Wang, A. Bochkovskiy and H.-Y. M. Liao. “YOLOv7: Trainable bag-of-freebies sets new state-of-the-art for real-time object detectors”. *arXiv* (2022).
- [4] C. Lyu and al. “RTMDet: An Empirical Study of Designing Real-Time Object Detectors”. *arXiv* (2022).
- [5] Y. Li, H. Mao, R. Girshick and K. He. “Exploring Plain Vision Transformer Backbones for Object Detection”. *arXiv* (2022).
- [6] N. Carion and al. “End-to-End Object Detection with Transformers”. *arXiv* (2020). DOI: [10.48550/arXiv.2005.12872](https://arxiv.org/abs/10.48550/arXiv.2005.12872).
- [7] W. Guimont-Martin, J.-M. Fortin, F. Pomerleau and P. Giguère. “MaskBEV: Joint Object Detection and Footprint Completion for Bird’s-eye View 3D Point Clouds”. *2023 IEEE/RSJ International Conference on Intelligent Robots and Systems (IROS)* (2023), pp. 5677–5684.
- [8] H. Law and J. Deng. “CornerNet: Detecting Objects as Paired Keypoints”. *ECCV* (2018).
- [9] N. Carion, F. Massa, and al. “End-to-End Object Detection with Transformers”. *ECCV* (2020).
- [10] X. Zhou, D. Wang, and P. Krähenbühl. “Objects as points”. *arXiv preprint arXiv:1904.07850* (2019).
- [11] Y. Zhao and al. “DETRs Beat YOLOs on Real-time Object Detection”. *arXiv* (2024).
- [12] Ashish Vaswani and al. “Attention is all you need”. *NIPS* (2017).
- [13] J. Redmon, S. Divvala, R. Girshick and A. Farhadi. “You Only Look Once: Unified, Real-Time Object Detection”. *arXiv* (2016).
- [14] Zheng Ge, Songtao Liu, Feng Wang, Zeming Li and Jian Sun. “YOLOX: Exceeding YOLO Series in 2021”. *arXiv* (2021).
- [15] J. Redmon and A. Farhadi. “YOLO9000: Better, Faster, Stronger”. *arXiv* (2016).
- [16] Ultralytics. *YOLOv5: A state-of-the-art real-time object detection system*. <https://docs.ultralytics.com>. Accessed: insert date here. 2021.
- [17] Wang, Chien-Yao and Yeh, I-Hau and Liao, Hong-Yuan Mark. “You only learn one representation: Unified network for multiple tasks”. *arXiv preprint arXiv:2105.04206* (2021).
- [18] Xiang Li and al. “Generalized Focal Loss: Learning Qualified and Distributed Bounding Boxes for Dense Object Detection”. *arXiv* (2020).
- [19] Hamid Rezaatofghi and al. “Generalized Intersection over Union: A Metric and A Loss for Bounding Box Regression”. *arXiv* (2019).
- [20] Hongyi Zhang, Moustapha Cisse, Yann N. Dauphin and David Lopez-Paz. “mixup: Beyond Empirical Risk Minimization”. *arXiv* (2018).
- [21] J. Redmon and A. Farhadi. “YOLOv3: An Incremental Improvement”. *arXiv* (2018).
- [22] Diederik P. Kingma and Jimmy Ba. “Adam: A Method for Stochastic Optimization”. *arXiv* (2017).
- [23] He, Kaiming and Zhang, Xiangyu and Ren, Shaoqing and Sun, Jian. “Deep residual learning for image recognition”. *Proceedings of the IEEE conference on computer vision and pattern recognition*. 2016, pp. 770–778.
- [24] Z. Liu and al. “Swin Transformer: Hierarchical Vision Transformer using Shifted Windows”. *arXiv* (2021). DOI: [10.48550/arXiv.2103.14030](https://arxiv.org/abs/10.48550/arXiv.2103.14030).
- [25] A. Dosovitskiy and al. “An Image is Worth 16x16 Words: Transformers for Image Recognition at Scale”. *arXiv* (2021). DOI: [10.48550/arXiv.2010.11929](https://arxiv.org/abs/10.48550/arXiv.2010.11929).
- [26] He, Kaiming and Gkioxari, Georgia and Dollár, Piotr and Girshick, Ross. “Mask r-cnn”. *Proceedings of the IEEE international conference on computer vision*. 2017, pp. 2961–2969.
- [27] Girshick, Ross. “Fast r-cnn”. *Proceedings of the IEEE international conference on computer vision*. 2015, pp. 1440–1448.
- [28] Zhu, Xizhou and Su, Wei and Lu, Lewei and Li, Bin and Wang, Xiaogang and Dai, Jifeng. “Deformable detr: Deformable transformers for end-to-end object detection”. *arXiv preprint arXiv:2010.04159* (2020).
- [29] Meng, Depu and Chen, Xiaokang and Fan, Ze and Zeng, Gang and Li, Houqiang and Yuan, Yuhui and Sun, Lei and Wang, Jingdong. “Conditional detr for fast training convergence”. *Proceedings of the IEEE/CVF international conference on computer vision*. 2021, pp. 3651–3660.

¹²<https://huggingface.co/>, consulted on April 28th 2024

¹³<https://norlab.ulaval.ca/>, consulted April 21st 2024

- [30] Liu, Shilong and Li, Feng and Zhang, Hao and Yang, Xiao and Qi, Xianbiao and Su, Hang and Zhu, Jun and Zhang, Lei. “Dab-detr: Dynamic anchor boxes are better queries for detr”. *arXiv preprint arXiv:2201.12329* (2022).
- [31] Sandler, Mark and Howard, Andrew and Zhu, Menglong and Zhmoginov, Andrey and Chen, Liang-Chieh. “Mobilenetv2: Inverted residuals and linear bottlenecks”. *Proceedings of the IEEE conference on computer vision and pattern recognition*. 2018, pp. 4510–4520.
- [32] Zhang, Hao and Li, Feng and Liu, Shilong and Zhang, Lei and Su, Hang and Zhu, Jun and Ni, Lionel M and Shum, Heung-Yeung. “Dino: Detr with improved denoising anchor boxes for end-to-end object detection”. *arXiv preprint arXiv:2203.03605* (2022).
- [33] Chen, Qiang and Wang, Yingming and Yang, Tong and Zhang, Xiangyu and Cheng, Jian and Sun, Jian. “You only look one-level feature”. *Proceedings of the IEEE/CVF conference on computer vision and pattern recognition*. 2021, pp. 13039–13048.
- [34] Lin, Tsung-Yi and Goyal, Priya and Girshick, Ross and He, Kaiming and Dollár, Piotr. “Focal loss for dense object detection”. *Proceedings of the IEEE international conference on computer vision*. 2017, pp. 2980–2988.
- [35] Kai Chen and al. “MMDetection: Open MMLab Detection Toolbox and Benchmark”. *arXiv* (2019).
- [36] K. He and al. “Masked Autoencoders Are Scalable Vision Learners”. *IEEE/CVF Conference on Computer Vision and Pattern Recognition* (2022), pp. 16000–16009.
- [37] Guimont-Martin, William. *transformer: flexible and easy to understand transformer models*. Version 0.1.0. Feb. 2023.
- [38] Yuxin Wu and al. “Detectron2”. *arXiv* (2019).
- [39] Golnaz Ghiasi and al. “Simple Copy-Paste is a Strong Data Augmentation Method for Instance Segmentation”. *arXiv* (2021).

Appendix

A Hyperparameters used

Table 7: List of used hyperparameters for implemented models.

Hyperparameter	YOLOv7	RTMDet	ViTDet	DETR
Optimizer	SGD	AdamW	AdamW	AdamW
Base Learning Rate	0.01	0.00125	0.0001	0.00001 for backbone 0.0001 for Transformer
Learning Rate Schedule	Sinusoidal ramp from 0.01 to 0.1	Flat (150 epochs) then Cosine	Multiplicative step of 0.1 for iterations 163889 to 177546	Multiplicative step of 0.1 after 200 epochs
Weight Decay	0.0005	0.05 (0 for bias and normalization)	0.01	0.0001
Optimizer Momentum	0.937	0.9	-	-
Batch size	64	80	24 (per GPU)	40
Dropout Rate	-	-	0.1	0.1
Maximum iterations	-	-	184375	-
Training Epochs	300	300	100	300
Warmup Iterations	3	1000	250	-
Warmup momentum	0.8	-	0.001	-
EMA Decay	-	0.9998	-	-
Input Size	640 × 640	640 × 640	1024 × 1024	-
Loss	BCELoss 5% box gain 30% cls gain 70% obj gain	QFL and GIoU	Classification: Cross-Entropy Bounding boxes: SmoothlLoss	l_1 loss with weight 5 GIoU loss with weight 2
Augmentation	Mosaic (100%) MixUp (15%) Copy paste (15%) Translation (20%) Scale (90%) Flip Left-Right (50%) HSV: 1.5% hue fraction 70% saturation fraction 40% value fraction	Mosaic and MixUp (first 280 epochs) LSJ([38], [39]) (last 20 epochs)	Mosaic and MixUp LSJ ([38], [39])	Crop and scale

B MMDetection pretrained model performances**Table 8:** Comparative frame per second performances (batch size of 1)

Model	Size (MiB)	TitanX	Quadro	A6000	RTX-3080	RTX-4090
Mask R-CNN R101	367.82	6.60	10.73	14.62	20.39	31.46
Mask R-CNN R50	295.17	7.89	12.69	19.69	21.25	37.70
Mask R-CNN X101	516.61	4.35	8.51	14.08	15.21	32.23
R-CNN Faster R50	161.72	9.31	13.26	14.66	26.11	34.01
Centernet R50	123.39	24.68	32.78	30.30	66.25	91.61
Cond. DETR R50	166.02	-	-	-	-	-
DAB DETR R50	166.99	-	-	-	-	-
Deform. DETR R50	153.24	-	-	-	-	-
D. DETR R50 (2 stages)	157.42	-	-	-	-	-
DETR R50	158.80	-	-	-	-	-
DINO-4 R50	182.17	-	-	-	-	-
DINO-5 Swin	836.67	-	-	-	-	-
Faster R-CNN Swin	380.91	7.18	14.24	24.77	27.51	61.00
Mask R-CNN Swin	182.54	15.80	25.11	30.21	39.04	73.12
Mask R-CNN Swin (Crop)	182.54	14.83	29.18	35.52	35.98	75.01
Retinanet	76.62	16.56	22.37	22.34	41.36	60.50
RTMDet-x	362.30	7.49	10.74	10.89	15.94	24.49
RTMDet-ins m	105.38	26.30	36.62	33.68	69.06	91.82
RTMDet-ins tiny	21.58	31.44	44.84	41.68	92.19	115.60
YOLOf R50	168.71	37.91	50.48	48.71	99.88	136.11
YOLOv3 d53	236.52	31.83	44.43	66.41	73.92	151.82
YOLOv3 MobileNetV2	14.41	50.39	69.21	66.20	154.00	208.64
YOLOX-l	207.06	28.98	39.33	36.36	59.36	107.36
YOLOX-s	34.30	41.49	54.37	54.39	110.49	142.14
YOLOX-tiny	19.35	40.60	54.47	53.27	111.78	149.90
YOLOX-x	378.31	18.17	24.09	38.23	41.08	76.39

Table 9: Comparative frame per second performances (batch size of 16).

Model	Size (MiB)	TitanX	Quadro	A6000	RTX-3080	RTX-4090
Mask R-CNN R101	367.82	0.36	0.88	1.55	1.45	2.45
Mask R-CNN R50	295.17	0.43	1.03	1.47	1.39	2.70
Mask R-CNN X101	516.61	0.25	0.67	1.23	1.16	2.09
R-CNN Faster R50	161.72	0.65	0.97	1.11	1.91	2.51
Centernet R50	123.39	2.62	3.73	5.15	5.25	8.92
Cond. DETR R50	166.02	-	-	-	-	-
DAB DETR R50	166.99	-	-	-	-	-
Deform. DETR R50	153.24	-	-	-	-	-
D. DETR R50 (2 stages)	157.42	-	-	-	-	-
DETR R50	158.80	-	-	-	-	-
DINO-4 R50	182.17	-	-	-	-	-
DINO-5 Swin	836.67	-	-	-	-	-
Faster R-CNN Swin	380.91	0.42	1.17	1.92	2.22	3.25
Mask R-CNN Swin	182.54	0.82	2.14	2.84	2.92	5.28
Mask R-CNN Swin (Crop)	182.54	0.94	2.21	2.89	2.56	5.25
Retinanet	76.62	1.48	2.53	3.41	3.58	5.61
RTMDet-x	362.30	0.53	0.72	0.83	1.02	1.55
RTMDet-ins m	105.38	2.25	3.62	4.43	5.32	8.48
RTMDet-ins tiny	21.58	3.89	6.25	6.34	9.16	13.62
YOLOf R50	168.71	3.92	5.45	7.54	8.75	12.49
YOLOv3 d53	236.52	2.86	4.13	6.08	6.01	9.73
YOLOv3 MobileNetV2	14.41	5.03	8.52	10.17	12.72	19.22
YOLOX-l	207.06	2.31	3.25	4.51	4.62	7.75
YOLOX-s	34.30	5.41	7.26	7.83	9.51	15.61
YOLOX-tiny	19.35	6.35	8.29	8.54	10.56	17.99
YOLOX-x	378.31	1.55	2.03	3.29	2.94	5.22

Table 10: Comparative frame per second performances (batch size of 32).

Model	Size (MiB)	TitanX	Quadro	A6000	RTX-3080	RTX-4090
Mask R-CNN R101	367.82	0.42	0.75	-	-	1.10
Mask R-CNN R50	295.17	0.52	0.89	-	-	1.42
Mask R-CNN X101	516.61	0.32	0.54	-	-	0.98
R-CNN Faster R50	161.72	0.50	0.61	-	-	1.22
Centernet R50	123.39	1.27	1.81	2.47	2.82	4.15
Cond. DETR R50	166.02	-	-	-	-	-
DAB DETR R50	166.99	-	-	-	-	-
Deform. DETR R50	153.24	-	-	-	-	-
D. DETR R50 (2 stages)	157.42	-	-	-	-	-
DETR R50	158.80	-	-	-	-	-
DINO-4 R50	182.17	-	-	-	-	-
DINO-5 Swin	836.67	-	-	-	-	-
Faster R-CNN Swin	380.91	0.2	0.63	1.09	1.01	1.73
Mask R-CNN Swin	182.54	0.43	1.12	1.43	1.50	2.48
Mask R-CNN Swin (Crop)	182.54	0.44	1.09	1.33	1.45	2.47
Retinanet	76.62	0.75	1.27	1.74	1.70	2.73
RTMDet-x	362.30	0.26	0.36	0.43	0.50	0.76
RTMDet-ins m	105.38	1.11	1.84	2.44	2.63	4.00
RTMDet-ins tiny	21.58	1.94	3.12	3.40	4.67	6.53
YOLOf R50	168.71	1.98	2.78	4.09	4.49	6.18
YOLOv3 d53	236.52	1.44	2.08	3.17	2.98	4.87
YOLOv3 MobileNetV2	14.41	2.52	4.25	5.11	6.39	9.01
YOLOX-l	207.06	1.17	1.65	2.35	2.39	3.77
YOLOX-s	34.30	2.70	3.64	4.08	4.82	7.60
YOLOX-tiny	19.35	3.18	4.13	4.36	5.14	8.66
YOLOX-x	378.31	0.78	1.08	1.68	1.47	2.47

Table 11: Accuracy performances for MMDetection pretrained networks.

Model	Size (MiB)	mAP	AP50	AP75	APs	APm	API
Mask R-CNN R101	367.82	0.46	0.64	0.50	0.28	0.49	0.59
Mask R-CNN R50	295.17	0.41	0.59	0.45	0.24	0.44	0.54
Mask R-CNN X101	516.61	0.47	0.65	0.51	0.29	0.50	0.60
R-CNN Faster R50	161.72	0.40	0.59	0.44	0.23	0.44	0.53
Centernet R50	123.39	0.40	0.58	0.44	0.23	0.45	0.52
Cond. DETR R50	166.02	0.41	0.62	0.44	0.20	0.44	0.60
DAB DETR R50	166.99	0.42	0.63	0.45	0.22	0.46	0.61
Deform. DETR R50	153.24	0.44	0.63	0.49	0.27	0.48	0.59
Deform. DETR R50 (2 stages)	157.42	0.47	0.66	0.51	0.30	0.50	0.62
DETR R50	158.80	0.40	0.60	0.42	0.18	0.44	0.59
DINO-4 R50	182.17	0.50	0.68	0.55	0.33	0.53	0.64
DINO-5 Swin	836.67	0.58	0.77	0.64	0.42	0.62	0.74
Faster R-CNN Swin	380.91	0.43	0.64	0.47	0.26	0.47	0.56
Mask R-CNN Swin	182.54	0.43	0.65	0.47	0.26	0.46	0.57
Mask R-CNN Swin (Crop)	182.54	0.46	0.68	0.50	0.30	0.49	0.60
Retinanet	76.62	0.40	0.60	0.43	0.22	0.45	0.56
RTMDet-x	362.30	0.53	0.70	0.58	0.36	0.57	0.69
RTMDet-ins m	105.38	0.49	0.67	0.53	0.30	0.54	0.65
RTMDet-ins tiny	21.58	0.40	0.58	0.44	0.21	0.45	0.58
YOLOf R50	168.71	0.38	0.57	0.40	0.19	0.42	0.53
YOLOv3 d53	236.52	0.28	0.49	0.28	0.10	0.30	0.44
YOLOv3 MobileNetV2	14.41	0.22	0.42	0.22	0.06	0.24	0.36
YOLOX-l	207.06	0.49	0.67	0.53	0.32	0.54	0.64
YOLOX-s	34.30	0.40	0.59	0.43	0.24	0.44	0.53
YOLOX-tiny	19.35	0.32	0.49	0.34	0.12	0.35	0.47
YOLOX-x	378.31	0.51	0.68	0.55	0.32	0.56	0.67

Table 12: Time performances, in seconds, for MMDet pretrained models with TitanX (batch size of 1).

Model	Size (MiB)	Time 1 mean	Time 1 std	Time 1 min	Time 1 median	Time 1 max
Mask R-CNN R101	367.822	0.151	0.005	0.137	0.151	0.176
Mask R-CNN R50	295.173	0.127	0.004	0.117	0.126	0.144
Mask R-CNN X101	516.609	0.230	0.010	0.212	0.226	0.262
R-CNN Faster R50	161.722	0.107	0.003	0.062	0.107	0.147
Centernet R50	123.391	0.041	0.001	0.039	0.041	0.072
Cond. DETR R50	166.023	-	-	-	-	-
DAB DETR R50	166.989	-	-	-	-	-
Deform. DETR R50	153.245	-	-	-	-	-
Deform. DETR R50 (2 stages)	157.421	-	-	-	-	-
DETR R50	158.799	-	-	-	-	-
DINO-4 R50	182.173	-	-	-	-	-
DINO-5 Swin	836.669	-	-	-	-	-
Faster R-CNN Swin	380.914	0.139	0.006	0.131	0.137	0.162
Mask R-CNN Swin	182.542	0.063	0.005	0.052	0.062	0.088
Mask R-CNN Swin (Crop)	182.542	0.067	0.007	0.053	0.066	0.094
Retinanet	76.619	0.060	0.002	0.058	0.060	0.087
RTMDet-x	362.298	0.133	0.004	0.126	0.132	0.156
RTMDet-ins m	105.383	0.038	0.001	0.035	0.038	0.052
RTMDet-ins tiny	21.579	0.032	0.001	0.029	0.032	0.047
YOLOf R50	168.715	0.026	0.001	0.025	0.027	0.040
YOLOv3 d53	236.519	0.031	0.001	0.029	0.031	0.039
YOLOv3 MobileNetV2	14.408	0.020	0.001	0.018	0.020	0.031
YOLOX-l	207.056	0.035	0.001	0.033	0.034	0.049
YOLOX-s	34.300	0.024	0.001	0.023	0.024	0.034
YOLOX-tiny	19.353	0.025	0.001	0.023	0.025	0.036
YOLOX-x	378.314	0.055	0.003	0.051	0.054	0.063

Table 13: Time performances, in seconds, for MMDet presets with TitanX (batch size of 16).

Model	Size (MiB)	Time 16 mean	Time 16 std	Time 16 min	Time 16 median	Time 16 max
Mask R-CNN R101	367.822	2.772	0.070	2.021	2.773	2.863
Mask R-CNN R50	295.173	2.320	0.064	2.121	2.324	2.485
Mask R-CNN X101	516.609	3.934	0.038	3.792	3.939	4.007
R-CNN Faster R50	161.722	1.543	0.023	1.471	1.539	1.609
Centernet R50	123.391	0.381	0.008	0.368	0.381	0.398
Cond. DETR R50	166.023	-	-	-	-	-
DAB DETR R50	166.989	-	-	-	-	-
Deform. DETR R50	153.245	-	-	-	-	-
Deform. DETR R50 (2 stages)	157.421	-	-	-	-	-
DETR R50	158.799	-	-	-	-	-
DINO-4 R50	182.173	-	-	-	-	-
DINO-5 Swin	836.669	-	-	-	-	-
Faster R-CNN Swin	380.914	2.387	0.096	2.185	2.422	2.533
Mask R-CNN Swin	182.542	1.216	0.040	0.991	1.221	1.301
Mask R-CNN Swin (Crop)	182.542	1.058	0.033	0.988	1.057	1.134
Retinanet	76.619	0.674	0.018	0.648	0.670	0.717
RTMDet-x	362.298	1.902	0.023	1.875	1.892	1.968
RTMDet-ins m	105.383	0.444	0.011	0.429	0.441	0.470
RTMDet-ins tiny	21.579	0.257	0.003	0.252	0.256	0.275
YOLOf R50	168.715	0.255	0.006	0.249	0.252	0.279
YOLOv3 d53	236.519	0.350	0.008	0.339	0.347	0.368
YOLOv3 MobileNetV2	14.408	0.199	0.005	0.195	0.197	0.219
YOLOX-l	207.056	0.433	0.013	0.420	0.427	0.459
YOLOX-s	34.300	0.185	0.002	0.182	0.184	0.193
YOLOX-tiny	19.353	0.158	0.001	0.156	0.157	0.162
YOLOX-x	378.314	0.644	0.018	0.616	0.647	0.666

Table 14: Time performances, in seconds, for MMDet presets with TitanX (batch size of 32).

Model	Size (MiB)	Time 32 mean	Time 32 std	Time 32 min	Time 32 median	Time 32 max
Mask R-CNN R101	367.822	-	-	-	-	-
Mask R-CNN R50	295.173	-	-	-	-	-
Mask R-CNN X101	516.609	-	-	-	-	-
R-CNN Faster R50	161.722	-	-	-	-	-
Centernet R50	123.391	0.788	0.020	0.763	0.782	0.822
Cond. DETR R50	166.023	-	-	-	-	-
DAB DETR R50	166.989	-	-	-	-	-
Deform. DETR R50	153.245	-	-	-	-	-
Deform. DETR R50 (2 stages)	157.421	-	-	-	-	-
DETR R50	158.799	-	-	-	-	-
DINO-4 R50	182.173	-	-	-	-	-
DINO-5 Swin	836.669	-	-	-	-	-
Faster R-CNN Swin	380.914	4.970	0.150	4.525	5.027	5.104
Mask R-CNN Swin	182.542	2.321	0.046	2.207	2.327	2.428
Mask R-CNN Swin (Crop)	182.542	2.288	0.046	2.186	2.282	2.401
Retinanet	76.619	1.335	0.041	1.279	1.322	1.396
RTMDet-x	362.298	3.787	0.022	3.749	3.784	3.890
RTMDet-ins m	105.383	0.897	0.027	0.857	0.896	0.949
RTMDet-ins tiny	21.579	0.516	0.010	0.503	0.514	0.549
YOLOf R50	168.715	0.505	0.012	0.489	0.504	0.526
YOLOv3 d53	236.519	0.695	0.017	0.670	0.702	0.718
YOLOv3 MobileNetV2	14.408	0.397	0.009	0.388	0.393	0.424
YOLOX-l	207.056	0.857	0.027	0.822	0.869	0.893
YOLOX-s	34.300	0.370	0.008	0.361	0.367	0.402
YOLOX-tiny	19.353	0.314	0.002	0.312	0.314	0.322
YOLOX-x	378.314	1.288	0.028	1.226	1.303	1.318

Table 15: Time performances, in seconds, for MMDet presets with Quadro (batch size of 1).

Model	Size (MiB)	Time 1 mean	Time 1 std	Time 1 min	Time 1 median	Time 1 max
Mask R-CNN R101	367.822	0.093	0.002	0.088	0.093	0.128
Mask R-CNN R50	295.173	0.079	0.002	0.073	0.079	0.092
Mask R-CNN X101	516.609	0.117	0.003	0.106	0.118	0.140
R-CNN Faster R50	161.722	0.075	0.002	0.042	0.075	0.098
Centernet R50	123.391	0.031	0.001	0.030	0.030	0.043
Cond. DETR R50	166.023	-	-	-	-	-
DAB DETR R50	166.989	-	-	-	-	-
Deform. DETR R50	153.245	-	-	-	-	-
Deform. DETR R50 (2 stages)	157.421	-	-	-	-	-
DETR R50	158.799	-	-	-	-	-
DINO-4 R50	182.173	-	-	-	-	-
DINO-5 Swin	836.669	-	-	-	-	-
Faster R-CNN Swin	380.914	0.070	0.002	0.063	0.070	0.082
Mask R-CNN Swin	182.542	0.040	0.004	0.031	0.039	0.052
Mask R-CNN Swin (Crop)	182.542	0.034	0.002	0.030	0.034	0.056
Retinanet	76.619	0.045	0.001	0.043	0.045	0.084
RTMDet-x	362.298	0.093	0.001	0.088	0.093	0.107
RTMDet-ins m	105.383	0.027	0.001	0.026	0.027	0.037
RTMDet-ins tiny	21.579	0.022	0.001	0.021	0.022	0.043
YOLOf R50	168.715	0.020	0.000	0.019	0.020	0.024
YOLOv3 d53	236.519	0.023	0.001	0.021	0.022	0.033
YOLOv3 MobileNetV2	14.408	0.014	0.000	0.014	0.014	0.023
YOLOX-l	207.056	0.025	0.001	0.024	0.025	0.038
YOLOX-s	34.300	0.018	0.001	0.018	0.018	0.027
YOLOX-tiny	19.353	0.018	0.001	0.018	0.018	0.037
YOLOX-x	378.314	0.042	0.001	0.037	0.042	0.049

Table 16: Time performances, in seconds, for MMDet presets with Quadro (batch size of 16).

Model	Size (MiB)	Time 16 mean	Time 16 std	Time 16 min	Time 16 median	Time 16 max
Mask R-CNN R101	367.822	1.133	0.014	1.105	1.132	1.215
Mask R-CNN R50	295.173	0.971	0.021	0.909	0.973	1.049
Mask R-CNN X101	516.609	1.495	0.018	1.451	1.495	1.555
R-CNN Faster R50	161.722	1.030	0.022	0.964	1.032	1.072
Centernet R50	123.391	0.268	0.002	0.265	0.268	0.276
Cond. DETR R50	166.023	-	-	-	-	-
DAB DETR R50	166.989	-	-	-	-	-
Deform. DETR R50	153.245	-	-	-	-	-
Deform. DETR R50 (2 stages)	157.421	-	-	-	-	-
DETR R50	158.799	-	-	-	-	-
DINO-4 R50	182.173	-	-	-	-	-
DINO-5 Swin	836.669	-	-	-	-	-
Faster R-CNN Swin	380.914	0.852	0.006	0.832	0.852	0.864
Mask R-CNN Swin	182.542	0.467	0.007	0.452	0.466	0.490
Mask R-CNN Swin (Crop)	182.542	0.453	0.006	0.439	0.452	0.478
Retinanet	76.619	0.396	0.003	0.389	0.396	0.405
RTMDet-x	362.298	1.381	0.008	1.361	1.381	1.417
RTMDet-ins m	105.383	0.276	0.002	0.272	0.276	0.281
RTMDet-ins tiny	21.579	0.160	0.001	0.157	0.160	0.169
YOLOf R50	168.715	0.183	0.001	0.181	0.183	0.186
YOLOv3 d53	236.519	0.242	0.001	0.240	0.242	0.244
YOLOv3 MobileNetV2	14.408	0.117	0.001	0.116	0.117	0.124
YOLOX-l	207.056	0.307	0.002	0.304	0.307	0.312
YOLOX-s	34.300	0.138	0.001	0.136	0.138	0.143
YOLOX-tiny	19.353	0.121	0.001	0.119	0.121	0.124
YOLOX-x	378.314	0.493	0.003	0.485	0.493	0.505

Table 17: Time performances, in seconds, for MMDet presets with Quadro (batch size of 32).

Model	Size (MiB)	Time 32 mean	Time 32 std	Time 32 min	Time 32 median	Time 32 max
Mask R-CNN R101	367.822	2.382	0.022	2.304	2.382	2.444
Mask R-CNN R50	295.173	1.906	0.046	1.780	1.907	2.008
Mask R-CNN X101	516.609	3.112	0.028	3.038	3.112	3.181
R-CNN Faster R50	161.722	1.999	0.042	1.865	1.999	2.099
Centernet R50	123.391	0.551	0.002	0.547	0.551	0.558
Cond. DETR R50	166.023	-	-	-	-	-
DAB DETR R50	166.989	-	-	-	-	-
Deform. DETR R50	153.245	-	-	-	-	-
Deform. DETR R50 (2 stages)	157.421	-	-	-	-	-
DETR R50	158.799	-	-	-	-	-
DINO-4 R50	182.173	-	-	-	-	-
DINO-5 Swin	836.669	-	-	-	-	-
Faster R-CNN Swin	380.914	1.583	0.019	1.564	1.578	1.674
Mask R-CNN Swin	182.542	0.894	0.007	0.879	0.894	0.914
Mask R-CNN Swin (Crop)	182.542	0.916	0.006	0.899	0.916	0.933
Retinanet	76.619	0.787	0.003	0.779	0.787	0.796
RTMDet-x	362.298	2.767	0.125	2.684	2.714	3.275
RTMDet-ins m	105.383	0.544	0.003	0.538	0.544	0.551
RTMDet-ins tiny	21.579	0.320	0.002	0.315	0.320	0.336
YOLOf R50	168.715	0.359	0.002	0.357	0.359	0.375
YOLOv3 d53	236.519	0.482	0.001	0.479	0.481	0.489
YOLOv3 MobileNetV2	14.408	0.235	0.001	0.234	0.235	0.239
YOLOX-l	207.056	0.606	0.002	0.602	0.606	0.613
YOLOX-s	34.300	0.275	0.002	0.273	0.275	0.290
YOLOX-tiny	19.353	0.242	0.001	0.240	0.242	0.245
YOLOX-x	378.314	0.926	0.004	0.916	0.925	0.935

Table 18: Time performances, in seconds, for MMDet presets with A6000 (batch size of 1).

Model	Size (MiB)	Time 1 mean	Time 1 std	Time 1 min	Time 1 median	Time 1 max
Mask R-CNN R101	367.822	0.068	0.013	0.056	0.064	0.194
Mask R-CNN R50	295.173	0.051	0.003	0.046	0.050	0.072
Mask R-CNN X100	516.609	0.071	0.012	0.060	0.067	0.213
R-CNN Faster R50	161.722	0.068	0.026	0.031	0.068	0.252
Centernet R50	123.391	0.033	0.009	0.026	0.030	0.143
Cond. DETR R50	166.023	-	-	-	-	-
DAB DETR R50	166.989	-	-	-	-	-
Deform. DETR R50	153.245	-	-	-	-	-
Deform. DETR R50 (2 stages)	157.421	-	-	-	-	-
DETR R50	158.799	-	-	-	-	-
DINO-4 R50	182.173	-	-	-	-	-
DINO-5 Swin	836.669	-	-	-	-	-
Faster R-CNN Swin	380.914	0.040	0.009	0.032	0.037	0.121
Mask R-CNN Swin	182.542	0.033	0.011	0.023	0.029	0.138
Mask R-CNN Swin (Crop)	182.542	0.028	0.005	0.023	0.027	0.076
Retinanet	76.619	0.045	0.009	0.037	0.042	0.145
RTMDet-x	362.298	0.092	0.021	0.074	0.084	0.197
RTMDet-ins m	105.383	0.030	0.006	0.023	0.027	0.140
RTMDet-ins tiny	21.579	0.024	0.005	0.018	0.022	0.071
YOLOf R50	168.715	0.021	0.005	0.016	0.019	0.089
YOLOv3 d53	236.519	0.015	0.002	0.012	0.015	0.051
YOLOv3 MobileNetV2	14.408	0.015	0.004	0.011	0.014	0.112
YOLOX-l	207.056	0.028	0.006	0.021	0.025	0.076
YOLOX-s	34.300	0.018	0.003	0.015	0.018	0.059
YOLOX-tiny	19.353	0.019	0.003	0.015	0.018	0.051
YOLOX-x	378.314	0.026	0.002	0.023	0.026	0.042

Table 19: Time performances, in seconds, for MMDet presets with A6000 (batch size of 16).

Model	Size (MiB)	Time 16 mean	Time 16 std	Time 16 min	Time 16 median	Time 16 max
Mask R-CNN R101	367.822	0.644	0.008	0.629	0.642	0.673
Mask R-CNN R50	295.173	0.679	0.013	0.638	0.678	0.709
Mask R-CNN X100	516.609	0.815	0.007	0.799	0.814	0.847
R-CNN Faster R50	161.722	0.904	0.042	0.791	0.900	1.104
Centernet R50	123.391	0.194	0.010	0.182	0.191	0.241
Cond. DETR R50	166.023	-	-	-	-	-
DAB DETR R50	166.989	-	-	-	-	-
Deform. DETR R50	153.245	-	-	-	-	-
Deform. DETR R50 (2 stages)	157.421	-	-	-	-	-
DETR R50	158.799	-	-	-	-	-
DINO-4 R50	182.173	-	-	-	-	-
DINO-5 Swin	836.669	-	-	-	-	-
Faster R-CNN Swin	380.914	0.521	0.009	0.508	0.519	0.560
Mask R-CNN Swin	182.542	0.351	0.013	0.332	0.349	0.422
Mask R-CNN Swin (Crop)	182.542	0.346	0.008	0.332	0.345	0.397
Retinanet	76.619	0.293	0.005	0.286	0.292	0.322
RTMDet-x	362.298	1.206	0.031	1.127	1.205	1.303
RTMDet-ins m	105.383	0.226	0.017	0.204	0.219	0.280
RTMDet-ins tiny	21.579	0.158	0.021	0.134	0.148	0.239
YOLOf R50	168.715	0.133	0.011	0.122	0.128	0.192
YOLOv3 d53	236.519	0.164	0.007	0.157	0.162	0.210
YOLOv3 MobileNetV2	14.408	0.098	0.012	0.088	0.093	0.154
YOLOX-l	207.056	0.222	0.006	0.214	0.220	0.247
YOLOX-s	34.300	0.128	0.016	0.116	0.121	0.190
YOLOX-tiny	19.353	0.117	0.015	0.105	0.112	0.204
YOLOX-x	378.314	0.304	0.003	0.300	0.302	0.316

Table 20: Time performances, in seconds, for MMDet presets with A6000 (batch size of 32).

Model	Size (MiB)	Time 32 mean	Time 32 std	Time 32 min	Time 32 median	Time 32 max
Mask R-CNN R101	367.822	1.341	0.012	1.313	1.339	1.383
Mask R-CNN R50	295.173	1.127	0.021	1.069	1.131	1.168
Mask R-CNN X100	516.609	1.848	0.016	1.817	1.845	1.933
R-CNN Faster R50	161.722	1.639	0.046	1.558	1.633	1.783
Centernet R50	123.391	0.405	0.012	0.388	0.404	0.448
Cond. DETR R50	166.023	-	-	-	-	-
DAB DETR R50	166.989	-	-	-	-	-
Deform. DETR R50	153.245	-	-	-	-	-
Deform. DETR R50 (2 stages)	157.421	-	-	-	-	-
DETR R50	158.799	-	-	-	-	-
DINO-4 R50	182.173	-	-	-	-	-
DINO-5 Swin	836.669	-	-	-	-	-
Faster R-CNN Swin	380.914	0.915	0.011	0.898	0.913	0.960
Mask R-CNN Swin	182.542	0.698	0.014	0.674	0.696	0.742
Mask R-CNN Swin (Crop)	182.542	0.753	0.019	0.714	0.752	0.822
Retinanet	76.619	0.574	0.007	0.564	0.572	0.611
RTMDet-x	362.298	2.351	0.071	2.226	2.347	2.665
RTMDet-ins m	105.383	0.410	0.013	0.394	0.405	0.448
RTMDet-ins tiny	21.579	0.294	0.016	0.270	0.289	0.361
YOLOf R50	168.715	0.244	0.008	0.234	0.243	0.270
YOLOv3 d53	236.519	0.316	0.009	0.303	0.313	0.347
YOLOv3 MobileNetV2	14.408	0.196	0.016	0.178	0.188	0.270
YOLOX-l	207.056	0.426	0.007	0.416	0.423	0.450
YOLOX-s	34.300	0.245	0.013	0.229	0.242	0.279
YOLOX-tiny	19.353	0.229	0.017	0.211	0.225	0.285
YOLOX-x	378.314	0.595	0.002	0.592	0.595	0.608

Table 21: Time performances, in seconds, for MMDet presets with RTX-3080Ti (batch size of 1).

Model	Size (MiB)	Time 1 mean	Time 1 std	Time 1 min	Time 1 median	Time 1 max
Mask R-CNN R101	367.822	0.049	0.002	0.046	0.049	0.095
Mask R-CNN R50	295.173	0.047	0.001	0.044	0.047	0.061
Mask R-CNN X101	516.609	0.066	0.002	0.061	0.065	0.092
R-CNN Faster R50	161.722	0.038	0.001	0.036	0.038	0.070
Centernet R50	123.391	0.015	0.001	0.015	0.015	0.034
Cond. DETR R50	166.023	-	-	-	-	-
DAB DETR R50	166.989	-	-	-	-	-
Deform. DETR R50	153.245	-	-	-	-	-
Deform. DETR R50 (2 stages)	157.421	-	-	-	-	-
DETR R50	158.799	-	-	-	-	-
DINO-4 R50	182.173	-	-	-	-	-
DINO-5 Swin	836.669	-	-	-	-	-
Faster R-CNN Swin	380.914	0.036	0.002	0.033	0.036	0.044
Mask R-CNN Swin	182.542	0.026	0.002	0.021	0.025	0.053
Mask R-CNN Swin (Crop)	182.542	0.028	0.006	0.021	0.026	0.079
Retinanet	76.619	0.024	0.001	0.023	0.024	0.037
RTMDet-x	362.298	0.063	0.003	0.059	0.062	0.122
RTMDet-ins m	105.383	0.014	0.001	0.013	0.014	0.039
RTMDet-ins tiny	21.579	0.011	0.001	0.010	0.011	0.024
YOLOf R50	168.715	0.010	0.001	0.010	0.010	0.027
YOLOv3 d53	236.519	0.014	0.000	0.013	0.013	0.022
YOLOv3 MobileNetV2	14.408	0.006	0.001	0.006	0.006	0.018
YOLOX-l	207.056	0.017	0.001	0.016	0.017	0.027
YOLOX-s	34.300	0.009	0.000	0.009	0.009	0.019
YOLOX-tiny	19.353	0.009	0.000	0.009	0.009	0.023
YOLOX-x	378.314	0.024	0.002	0.023	0.024	0.047

Table 22: Time performances, in seconds, for MMDet presets with RTX-3080Ti (batch size of 16).

Model	Size (MiB)	Time 16 mean	Time 16 std	Time 16 min	Time 16 median	Time 16 max
Mask R-CNN R101	367.822	0.690	0.009	0.665	0.690	0.767
Mask R-CNN R50	295.173	0.721	0.046	0.649	0.712	1.007
Mask R-CNN X101	516.609	0.860	0.103	0.784	0.825	1.321
R-CNN Faster R50	161.722	0.524	0.011	0.490	0.524	0.597
Centernet R50	123.391	0.190	0.003	0.188	0.190	0.219
Cond. DETR R50	166.023	-	-	-	-	-
DAB DETR R50	166.989	-	-	-	-	-
Deform. DETR R50	153.245	-	-	-	-	-
Deform. DETR R50 (2 stages)	157.421	-	-	-	-	-
DETR R50	158.799	-	-	-	-	-
DINO-4 R50	182.173	-	-	-	-	-
DINO-5 Swin	836.669	-	-	-	-	-
Faster R-CNN Swin	380.914	0.451	0.016	0.426	0.446	0.513
Mask R-CNN Swin	182.542	0.343	0.025	0.313	0.336	0.498
Mask R-CNN Swin (Crop)	182.542	0.390	0.027	0.350	0.384	0.504
Retinanet	76.619	0.279	0.010	0.267	0.275	0.324
RTMDet-x	362.298	0.985	0.049	0.925	0.980	1.109
RTMDet-ins m	105.383	0.188	0.002	0.185	0.188	0.202
RTMDet-ins tiny	21.579	0.109	0.002	0.105	0.109	0.124
YOLOf R50	168.715	0.114	0.003	0.111	0.113	0.137
YOLOv3 d53	236.519	0.167	0.003	0.164	0.166	0.208
YOLOv3 MobileNetV2	14.408	0.079	0.002	0.077	0.079	0.102
YOLOX-l	207.056	0.216	0.006	0.212	0.213	0.261
YOLOX-s	34.300	0.105	0.001	0.104	0.105	0.126
YOLOX-tiny	19.353	0.095	0.001	0.094	0.095	0.108
YOLOX-x	378.314	0.341	0.015	0.329	0.333	0.404

Table 23: Time performances, in seconds, for MMDet presets with RTX-3080Ti (batch size of 32).

Model	Size (MiB)	Time 32 mean	Time 32 std	Time 32 min	Time 32 median	Time 32 max
Mask R-CNN R101	367.822	-	-	-	-	-
Mask R-CNN R50	295.173	-	-	-	-	-
Mask R-CNN X101	516.609	-	-	-	-	-
R-CNN Faster R50	161.722	-	-	-	-	-
Centernet R50	123.391	0.355	0.004	0.350	0.354	0.376
Cond. DETR R50	166.023	-	-	-	-	-
DAB DETR R50	166.989	-	-	-	-	-
Deform. DETR R50	153.245	-	-	-	-	-
Deform. DETR R50 (2 stages)	157.421	-	-	-	-	-
DETR R50	158.799	-	-	-	-	-
DINO-4 R50	182.173	-	-	-	-	-
DINO-5 Swin	836.669	-	-	-	-	-
Faster R-CNN Swin	380.914	0.994	0.015	0.955	0.994	1.038
Mask R-CNN Swin	182.542	0.666	0.046	0.613	0.652	0.879
Mask R-CNN Swin (Crop)	182.542	0.690	0.055	0.636	0.675	0.941
Retinanet	76.619	0.587	0.037	0.528	0.583	0.654
RTMDet-x	362.298	1.984	0.062	1.886	1.969	2.184
RTMDet-ins m	105.383	0.380	0.004	0.375	0.378	0.406
RTMDet-ins tiny	21.579	0.214	0.002	0.210	0.214	0.237
YOLOf R50	168.715	0.223	0.001	0.222	0.223	0.227
YOLOv3 d53	236.519	0.336	0.008	0.324	0.337	0.359
YOLOv3 MobileNetV2	14.408	0.156	0.005	0.154	0.156	0.212
YOLOX-l	207.056	0.419	0.002	0.417	0.418	0.441
YOLOX-s	34.300	0.207	0.002	0.206	0.207	0.217
YOLOX-tiny	19.353	0.195	0.007	0.188	0.189	0.217
YOLOX-x	378.314	0.678	0.028	0.649	0.667	0.777

Table 24: Time performances, in seconds, for MMDet presets with RTX-4090 (batch size of 1).

Model	Size (MiB)	Time 1 mean	Time 1 std	Time 1 min	Time 1 median	Time 1 max
Mask R-CNN R101	367.822	0.032	0.002	0.029	0.031	0.049
Mask R-CNN R50	295.173	0.027	0.001	0.025	0.026	0.039
Mask R-CNN X100	516.609	0.030	0.001	0.028	0.030	0.045
R-CNN Faster R50	161.722	0.029	0.002	0.017	0.029	0.057
Centernet R50	123.391	0.011	0.001	0.010	0.011	0.023
Cond. DETR R50	166.023	-	-	-	-	-
DAB DETR R50	166.989	-	-	-	-	-
Deformable DETR R50	153.245	-	-	-	-	-
Deformable DETR R50 (2 stages)	157.421	-	-	-	-	-
DETR R50	158.799	-	-	-	-	-
DINO-4 R50	182.173	-	-	-	-	-
DINO-5 Swin	836.669	-	-	-	-	-
Faster R-CNN Swin	380.914	0.016	0.001	0.015	0.016	0.030
Mask R-CNN Swin	182.542	0.014	0.001	0.012	0.013	0.025
Mask R-CNN Swin (Crop)	182.542	0.013	0.001	0.012	0.014	0.024
Retinanet	76.619	0.017	0.001	0.015	0.016	0.032
RTMDet-x	362.298	0.041	0.001	0.040	0.041	0.067
RTMDet-ins m	105.383	0.011	0.002	0.010	0.010	0.024
RTMDet-ins tiny	21.579	0.009	0.001	0.008	0.008	0.020
YOLOf R50	168.715	0.007	0.001	0.007	0.007	0.016
YOLOv3 d53	236.519	0.007	0.000	0.006	0.007	0.013
YOLOv3 MobileNetV2	14.408	0.005	0.000	0.005	0.005	0.012
YOLOX-l	207.056	0.009	0.001	0.009	0.009	0.020
YOLOX-s	34.300	0.007	0.001	0.006	0.007	0.017
YOLOX-tiny	19.353	0.007	0.001	0.006	0.006	0.016
YOLOX-x	378.314	0.013	0.001	0.013	0.013	0.025

Table 25: Time performances, in seconds, for MMDet presets with RTX-4090 (batch size of 16).

Model	Size (MiB)	Time 16 mean	Time 16 std	Time 16 min	Time 16 median	Time 16 max
Mask R-CNN R101	367.822	0.409	0.014	0.389	0.403	0.448
Mask R-CNN R50	295.173	0.370	0.010	0.349	0.367	0.405
Mask R-CNN X100	516.609	0.478	0.012	0.466	0.473	0.531
R-CNN Faster R50	161.722	0.398	0.007	0.379	0.400	0.416
Centernet R50	123.391	0.112	0.002	0.111	0.111	0.122
Cond. DETR R50	166.023	-	-	-	-	-
DAB DETR R50	166.989	-	-	-	-	-
Deformable DETR R50	153.245	-	-	-	-	-
Deformable DETR R50 (2 stages)	157.421	-	-	-	-	-
DETR R50	158.799	-	-	-	-	-
DINO-4 R50	182.173	-	-	-	-	-
DINO-5 Swin	836.669	-	-	-	-	-
Faster R-CNN Swin	380.914	0.307	0.010	0.286	0.305	0.338
Mask R-CNN Swin	182.542	0.190	0.004	0.180	0.189	0.205
Mask R-CNN Swin (Crop)	182.542	0.190	0.003	0.185	0.190	0.199
Retinanet	76.619	0.178	0.002	0.175	0.178	0.188
RTMDet-x	362.298	0.646	0.026	0.622	0.632	0.758
RTMDet-ins m	105.383	0.118	0.003	0.114	0.117	0.131
RTMDet-ins tiny	21.579	0.073	0.003	0.070	0.073	0.085
YOLOf R50	168.715	0.080	0.003	0.078	0.078	0.091
YOLOv3 d53	236.519	0.103	0.004	0.098	0.102	0.114
YOLOv3 MobileNetV2	14.408	0.052	0.002	0.051	0.051	0.060
YOLOX-l	207.056	0.129	0.004	0.126	0.127	0.141
YOLOX-s	34.300	0.064	0.003	0.060	0.064	0.074
YOLOX-tiny	19.353	0.056	0.002	0.054	0.055	0.063
YOLOX-x	378.314	0.192	0.006	0.187	0.189	0.223

Table 26: Time performances, in seconds, for MMDet presets with RTX-4090 (batch size of 32).

Model	Size (MiB)	Time 32 mean	Time 32 std	Time 32 min	Time 32 median	Time 32 max
Mask R-CNN R101	367.822	0.909	0.028	0.864	0.906	0.987
Mask R-CNN R50	295.173	0.702	0.021	0.678	0.697	0.854
Mask R-CNN X100	516.609	1.020	0.032	0.980	1.007	1.096
R-CNN Faster R50	161.722	0.823	0.008	0.809	0.821	0.901
Centernet R50	123.391	0.241	0.002	0.240	0.241	0.251
Cond. DETR R50	166.023	-	-	-	-	-
DAB DETR R50	166.989	-	-	-	-	-
Deformable DETR R50	153.245	-	-	-	-	-
Deformable DETR R50 (2 stages)	157.421	-	-	-	-	-
DETR R50	158.799	-	-	-	-	-
DINO-4 R50	182.173	-	-	-	-	-
DINO-5 Swin	836.669	-	-	-	-	-
Faster R-CNN Swin	380.914	0.577	0.020	0.557	0.567	0.632
Mask R-CNN Swin	182.542	0.403	0.007	0.389	0.402	0.425
Mask R-CNN Swin (Crop)	182.542	0.405	0.007	0.389	0.404	0.425
Retinanet	76.619	0.366	0.007	0.360	0.364	0.414
RTMDet-x	362.298	1.310	0.027	1.269	1.309	1.411
RTMDet-ins m	105.383	0.250	0.004	0.243	0.249	0.269
RTMDet-ins tiny	21.579	0.153	0.002	0.151	0.153	0.163
YOLOf R50	168.715	0.162	0.004	0.158	0.160	0.175
YOLOv3 d53	236.519	0.205	0.005	0.200	0.204	0.232
YOLOv3 MobileNetV2	14.408	0.111	0.004	0.108	0.109	0.124
YOLOX-l	207.056	0.265	0.002	0.264	0.265	0.283
YOLOX-s	34.300	0.132	0.004	0.126	0.130	0.144
YOLOX-tiny	19.353	0.115	0.003	0.112	0.114	0.127
YOLOX-x	378.314	0.406	0.009	0.397	0.402	0.440